

# Electric double-layer capacitors with tea waste derived activated carbon electrodes and plastic crystal based flexible gel polymer electrolytes

M Suleman<sup>1</sup>, M Deraman<sup>1,\*</sup>, M A R Othman<sup>1</sup>, R Omar<sup>1</sup>, M A Hashim<sup>2</sup>, N H Basri<sup>1</sup>, N S M Nor<sup>1</sup>, B N M Dolah<sup>1</sup>, M F Y M Hanappi<sup>1</sup>, E Hamdan<sup>1</sup>, N E S Sazali<sup>1</sup>, N S M Tajuddin<sup>1</sup> and M R M Jasni<sup>1</sup>

<sup>1</sup>School of Applied Physics, Faculty of Science and Technology, National University of Malaysia, 43600, Bangi, Selangor, Malaysia

<sup>2</sup>Faculty of Science and Technology, Universiti Sains Islam Malaysia, Bandar Baru Nilai, 71800 Nilai, Negeri Sembilan, Malaysia

E-mail: \*madra@ukm.edu.my/mderaman113@gmail.com

**Abstract.** We report a novel configuration of symmetrical electric double-layer capacitors (EDLCs) comprising a plastic crystalline succinonitrile (SN) based flexible polymer gel electrolyte, incorporated with sodium trifluoromethane sulfonate (NaTf) immobilised in a host polymer poly (vinylidene fluoride-co-hexafluoropropylene) (PVdF-HFP). The cost-effective activated carbon powder possessing a specific surface area (SSA) of  $\sim 1700 \text{ m}^2\text{g}^{-1}$  containing a large proportion of meso-porosity has been derived from tea waste to use as supercapacitor electrodes. The high ionic conductivity ( $\sim 3.6 \times 10^{-3} \text{ S cm}^{-1}$  at room temperature) and good electrochemical stability render the gel polymer electrolyte film a suitable candidate for the fabrication of EDLCs. The performance of the EDLCs has been tested by electrochemical impedance spectroscopy (EIS), cyclic voltammetry (CV), and galvanostatic charge-discharge studies. The performance of the EDLC cell is found to be promising in terms of high values of specific capacitance ( $\sim 270 \text{ F g}^{-1}$ ), specific energy ( $\sim 36 \text{ Wh kg}^{-1}$ ), and power density ( $\sim 33 \text{ kW kg}^{-1}$ ).

## 1. Introduction

Electrical double-layer capacitors (EDLCs), also referred as electrochemical supercapacitors, belong to an emerging class of power sources, which employ various forms of carbon such as activated carbon powder/fibres/fabrics, CNTs, graphene etc., as an electrode material [1]. These are potential energy storage devices because they offer high specific capacitance, higher specific energy than electrolytic capacitors, higher power density and longer cycle life than rechargeable batteries [1-4]. Of the variety of forms of carbons, the activated carbons have been most widely investigated materials [5]. The surface area and porosity of these materials can be tailored by utilising different precursors and preparation methods [6]. The activated carbons containing large proportion of micro-porosity that results in larger surface area ( $\sim 1000\text{-}2500 \text{ m}^2 \text{ g}^{-1}$ ), have the ability to offer larger value of specific capacitance ( $100\text{-}350 \text{ F g}^{-1}$ ) as compared to low surface area meso-porous carbons e.g. CNTs, CNFs, fullerene, graphene, etc. [5]. Further, the micro-porous activated carbons, offer high specific



capacitance values but with poor rate capability and cycle life [7,8], whereas, the meso-porous carbons offer the excellent rate capability [9,10-12]. Therefore, the carbon electrodes containing large proportion of meso-porosity along with their micro-porous texture are essentially required to fabricate EDLCs offering larger specific capacitance with high rate performance. In this race, the preparation of activated carbons derived from natural resources, e.g. oil palm empty fruit bunches [13-16], rubber wood saw dust [17], coconut shell [18-20], etc., is a cost-effective approach.

Owing to various limitations including leakage of electrolytes, bulky design, corrosion of electrodes, etc., liquid electrolytes have been replaced by gel polymer electrolytes (GPEs) flexible films. The gel polymer electrolytes (GPEs) provide the solid like mechanical properties along with high ionic conductivity, almost comparable to that of liquid electrolytes [4,21,22]. Further, in recent years, few polymer-based electrolytes are reported incorporating plastic crystalline material succinonitrile (SN) as solid solvent/plasticizer to replace organic solvents or ionic liquids (ILs) [23-28]. SN is a waxy solid having disc like molecules with short range rotational disorder but long range translational order, whose plastic crystal phase extends over a temperature range from  $\sim -40$  to  $\sim 57$  °C [29,30]. In its plastic crystalline phase, the molecules of SN perform rotational motion about central C-C bond which increases the mobility of the ions according to the paddle-wheel or revolving door mechanism that result in enhanced ionic conductivity [24,29,30]. Furthermore, due to its high polarity (giving a dielectric constant ( $\epsilon$ )  $\sim 55$  at room temperature) and high diffusivity, it can dissociate salts into free ions [29]. Therefore, in addition to exhibiting high ionic conductivity, the GPEs incorporating SN have excellent properties such as non-volatile and less flammable character as compared to liquid organic solvents like acetonitrile, etc., and ability of proper electrode-electrolyte contacts in devices and safety concern.

In this communication, we report a novel configuration of the solid-state symmetric EDLCs with tea waste derived activated carbon (tw-AC) electrodes and flexible GPE films comprising of solutions of sodium trifluoromethane sulfonate (NaTf) in a plastic crystal succinonitrile (SN) and a host polymer poly (vinylidene fluoride-co-hexafluoropropylene) (PVdF-HFP). The characteristics of the EDLCs were evaluated by electrochemical impedance spectroscopy (EIS), cyclic voltammetry (CV), and galvanostatic charge-discharge tests. The experimental results are discussed in terms of characteristics of the gel polymer electrolytes, ionic sizes and porous properties of the carbon electrodes.

## 2. Experimental

### 2.1. Preparation of GPE film

The SN, the sodium salt (NaTf) and the polymer poly (vinylidene fluoride-hexafluoropropylene) (PVdFHFP) (molecular mass  $\approx 400\ 000$ ) were purchased from Sigma–Aldrich and used as received. The sodium salt was vacuum dried at  $\sim 80$  °C for 12 h to evaporate absorbed moisture. The other materials, namely PVdF-HFP and SN, were vacuum dried at room temperature. The GPE films were prepared by solution-cast method. Briefly, 5 mol% solution of NaTf in SN was prepared separately in a common solvent acetone. This solution was added to the host polymer, PVdF-HFP (separately dissolved in acetone; 1 g in 15 mL) in a weight ratio of 80:20. This mixture was then stirred magnetically at room temperature for  $\sim 24$  h.

The final viscous solution was cast over glass petri-dish and left for slow evaporation of common solvent acetone at room temperature. Finally, the semi-transparent, free-standing and flexible GPE film of thickness  $\sim 100$ - $150$   $\mu\text{m}$  was obtained. The GPE film was stored in an argon atmosphere to avoid moisture adsorption. A photograph of a typical composition of GPE film, showing its flexible nature, is depicted in figure 1. However, the viscous solution of GPE film in acetone, stored in dry atmosphere, was used to fabricate EDLC cells. The following composition of GPE film was used as separator/electrolyte in EDLC cells: PVdF-HFP/SN/NaTf (SN-SALT-GPE). The films of the gel electrolytes were used for their electrochemical characterization.

### 2.2. Preparation of activated carbon powder and the electrodes

The activated carbon powder was prepared from tea waste using the process reported elsewhere [18]. Briefly, at first, the tea waste was thoroughly ground to form a powder. A slurry was prepared by a thorough mixing of the powder and an activating agent zinc chloride with a ratio of 1:2 w/w in the presence of de-ionized water in a mortar and pestle. This slurry was dried overnight at  $\sim 110$  °C in vacuum. The mixture so obtained was then heated by increasing the temperature from 25 °C to 800 °C at a rate of 5 °C  $\text{min}^{-1}$  under the constant flow of nitrogen gas. Then the material was exposed to the constant flow of carbon dioxide gas maintaining the temperature at  $\sim 800$  °C for 2 h. After cooling down to room temperature, the powder was washed first by dilute HCl solution to dissolve and to remove zinc compounds, followed by washing with hot de-ionized water to make the powder free from chloride ions. The resulting tea waste carbon powder was dried overnight at  $\sim 110$  °C in vacuum.

To prepare supercapacitor electrodes, a slurry of the tw-AC powder, a conductive additive acetylene black (AB; Denka, Japan) and a binder PVdF-HFP (75:20:5 w/w) was prepared in a common solvent acetone by thorough mixing in a mortar and pestle. The slurry was coated on the flexible graphite sheets using a spin coater. The thickness of the electrode material on the graphite sheet was kept  $\sim 200$   $\mu\text{m}$  and the area of the electrode was  $\sim 1$   $\text{cm}^2$ . The mass of the activated carbon composite in the electrode was  $\sim 1$   $\text{mg cm}^{-2}$ . The prepared electrodes were vacuum-dried overnight at  $\sim 100$  °C before using them to fabricate EDLCs.

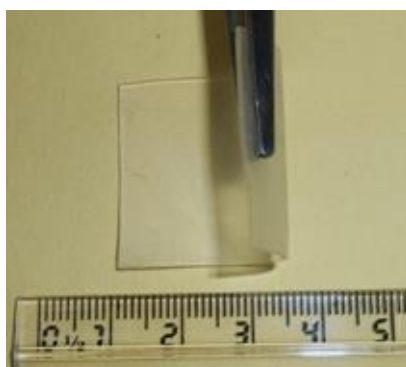


**Figure 1.** Photograph of a typical flexible GPE film.

### 2.3. Fabrication of EDLC cells

The GPE solution was spin coated on the surface of tw-AC electrodes coated on flexible graphite sheet (current collector) followed by drying to obtain a thin film of GPE over the surface of tw-AC electrodes. These three layer systems were assembled to form symmetric supercapacitor cells.

### 2.4. Instrumentation

The ionic conductivity of the GPE films was evaluated by EIS technique. The EIS measurement was carried out on the cell SS|GPE|SS (SS: stainless steel) in the frequency range from 1 Hz to 10 MHz using a Broadband Dielectric/Impedance Analyser (C-50 Alpha A, Novocontrol, Germany). The  $\text{N}_2$ -adsorption-desorption experiment for the measurement of specific surface area and other porosity parameters of the tw-AC powder was performed using a surface area and pore size analyzer (Micromeritics, USA). The powder samples were heated at  $\sim 300$  °C for 1 h in nitrogen atmosphere before the porosity measurements.

The performance of the EDLCs was evaluated using EIS, CV and galvanostatic charge-discharge methods. The EIS measurements were carried out using the Solartron 1260 A Impedance/Gain-Phase Analyser in the frequency range from 10 mHz to 100 kHz. The CV measurements were performed with the help of an electrochemical analyzer, mentioned above. The galvanostatic charge-discharge

characteristics of the capacitor cells were evaluated using a charge-discharge unit (model: BT-2000, Arbin Instruments, USA).

The capacitance values of the EDLC cells were evaluated using the following expressions, respectively, on the basis of EIS, CV and charge-discharge tests:

$$C = -\frac{1}{2\pi f Z''} \quad (1)$$

$$C = \frac{i}{s} \quad (2)$$

$$C = \frac{i\Delta t}{\Delta V} \quad (3)$$

where  $f$  is the frequency of applied a.c. voltage and  $Z''$  is the imaginary part of the total complex impedance,  $Z$ ,  $i$  is the current ( $i$  is constant for galvanostatic charge-discharge),  $s$  is the scan rate of the applied ramp voltage, and  $\Delta t$  is the time interval for the voltage change of  $\Delta V$  across the capacitor cells.

### 3. Results and discussion

#### 3.1. Electrochemical properties of GPE film

The solid plasticizer, SN is an insulator and its electrical conductivity is reported to be  $\sim 10^{-7}$  S  $\text{cm}^{-1}$  at room temperature, which is due to the presence of impurities in pure SN [31]. The GPE film, SN-SALT-GPE (PVdF-HFP/SN/SALT) offers a room temperature (25 °C) ionic conductivity ( $\sigma$ ) of  $\sim 3.6 \times 10^{-3}$  S  $\text{cm}^{-1}$ . Here SN has an important contribution to the ionic conductivity enhancement of GPE film and providing plasticizing ability to the GPE film that results in the reduction of electrode-electrolyte interfacial resistance. The host polymer PVdF-HFP, after immobilising the SN/SALT system provides excellent dimensional stability to the electrolytes to form free-standing GPE films.

Another important parameter associated with the electrolytes is their working voltage range over which an electrolyte remains safe and stable and generally referred as electrochemical stability window (ESW). The ESW value of the NaTf/NaTf based-GPE film has been reported in the range from  $\sim -2$  to  $+2$  V [32]. This working voltage range (ESW) is high enough to use the GPE film as solid-state-like electrolyte/separator in high performance supercapacitors/EDLCs.

#### 3.2. Surface area and porosity of electrode material

Figure 2 presents the  $\text{N}_2$ -adsorption-desorption isotherm and pore size distribution of the tw-AC powder. According to the IUPAC classification, the material shows a combination of Type I and Type IV isotherms [33] which indicates that the tw-AC electrode materials are porous containing both micro-pores and meso-pores. The pore size distribution of the tw-AC powder, calculated using the Barrett-Joyner-Halenda (BJH) method [34] with desorption data in figure 2, shows that the majority of the pores present in the electrode material have diameter  $< 4$  nm. A quantitative estimation of the BET surface area, micro- and meso-pore areas, and average pore size are presented in Table 1. The total pore volume has been estimated at the relative pressure of  $\sim 0.95$ . The presence of micro-pores and meso-pores in the electrodes leads to the enhanced performance characteristics of EDLCs, discussed later.

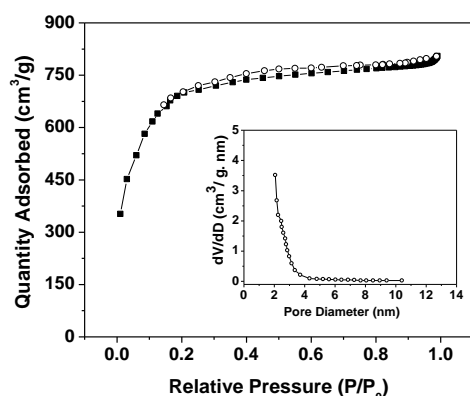


**Figure 2.** N<sub>2</sub>-adsorption-desorption isotherm of AC powder; and the corresponding pore size distribution curve (as inset).

**Table 1.** Specific surface area and porosity parameters of the AC powder evaluated from N<sub>2</sub>-adsorption-desorption isotherm.

$S_{\text{BET}}$ ( $\text{m}^2 \text{g}^{-1}$ )	$S_{\text{micro}}$ ( $\text{m}^2 \text{g}^{-1}$ )	$S_{\text{meso}}$ ( $\text{m}^2 \text{g}^{-1}$ )	$S_{\text{meso}}/S_{\text{micro}}$	$V_{\text{T}}$ ( $\text{cm}^3 \text{g}^{-1}$ )	$D_{\text{p}}$ (nm)
~ 1700	~ 620	~ 1080	1.88	0.98	~ 2.06

### 3.3. Characterization of EDLCs

As mentioned in the previous section, the symmetric EDLC cell, comprising of tw-AC based-electrodes and sodium ion conducting SN-based GPE, has been fabricated in two-electrode configuration. The electrochemical performance of the cells has been tested using the EIS, CV and galvanostatic charge-discharge tests for numerous cycles, as discussed in the following sections.

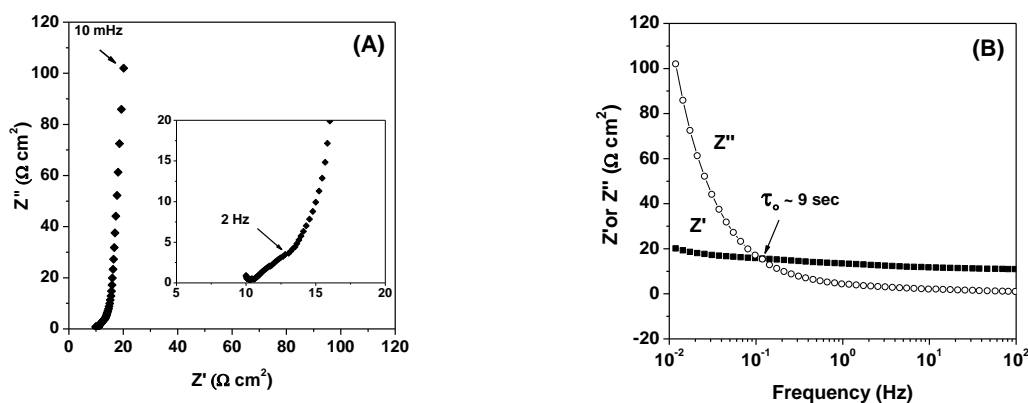
### 3.4. EIS analysis

Figure 3 (A) presents the Nyquist plot of the present EDLC cell obtained with PVdF-HFP/SN/SALT GPE film in the frequency range from 100 kHz to 10 mHz, with a magnified view of high frequency region in the inset. The approximate vertical slop at low frequency region displays the nearly ideal capacitive behaviour of cell up to a frequency of 2 Hz. Various electrical parameters of the device associated with the bulk properties of electrolytes and electrode-electrolyte interfaces have been evaluated using EIS measurements in different frequency regions. The specific capacitance (calculated at 10 mHz) was evaluated using equation (1). A capacitance value of ~ 270  $\text{Fg}^{-1}$  of tw-AC based electrode has been estimated for the present EDLC cell. Further, it can be observed from the magnified view of the impedance plot (figure 3(A), inset) that the plot has almost no signs of semicircle at high frequencies, implying the fast ion diffusion in the electrodes [35], whereas, a line intersecting the real axis at around  $-45^\circ$  has been observed which implies the porous nature of the electrodes.

The equivalent series resistance (*ESR*) of the device which represents the effective resistance contributed by the bulk resistance of the electrolyte, the intrinsic resistance of the active electrode material, and the contact resistance of the interface between active electrode material and current collector [36] can be evaluated by extrapolating the vertical portion of the plot [37]. The values of *ESR* are listed in Table 2. The tw-AC electrode interfaced with the GPE film exhibits an *ESR* of 15  $\Omega \text{cm}^2$ , which is comparable to the recently reported values for solid-state supercapacitors [20,38,39].

The impedance analysis has been extended to evaluate the rate capability (power delivering ability) of the EDLCs, in terms of the knee frequency ( $f_k$ , the maximum frequency at which capacitive behaviour is dominant i.e. the frequency from where the impedance curve starts rising steeply), and the characteristic response time  $\tau_0$  according to the Miller's approach [40]. For this purpose, the real and imaginary parts of impedance  $Z$  ( $Z'$  and  $Z''$ ) have been plotted against frequency. The typical plot (also referred as Bode plot) for the present cell is shown in figure 3(B). In this plot, the point of intersection of  $Z'$  and  $Z''$  (at which the impedance has a  $-45^\circ$  phase angle) gives the resonant

(response) frequency  $f_0$ ; the reciprocal of which gives the characteristic response time  $\tau_0$  as marked on figure 3(B). The values of  $f_k$  and  $\tau_0$  for the present EDLC cell have been estimated to be  $\sim 2$  Hz and  $\sim 9$  s, respectively.



**Figure 3.** (A) Nyquist plot of the solid-state EDLC cell, recorded at room temperature in the frequency range from 100 kHz to 10 mHz. The expanded representation of impedance plot in high frequency region is shown as inset; and (B) the corresponding Bode plot ( $Z'$  or  $Z''$  Versus  $\log f$ ).

**Table 2.** Various electrical parameters of EDLC cell evaluated from the Nyquist and Bode plots.

ESR ( $\Omega \text{ cm}^2$ )	C ( $\text{F g}^{-1}$ )	$f_0$ (Hz)	$\tau_0$ (s)	Knee Freq. (Hz)
$\sim 15$	$\sim 270$	$\sim 0.11$	$\sim 9$	$\sim 2$

### 3.5. Cyclic voltammetry

The electrochemical behaviour of the supercapacitor cell has been tested by the CV measurements performed in two electrode configuration. Figure 4(A) shows the CV profiles of the EDLC cell under investigation for different scan rates. The scan rate dependence of the capacitance values, evaluated using equation (2), are depicted in figure 4(B). It may be noted that with increasing the scan rates, the shapes of the voltammetric curves remain rectangular up to  $200 \text{ mV s}^{-1}$ , which indicate the proper formation of electric double-layer and fast switching behaviour of ions through the pores of tw-AC electrodes at the electrode-electrolyte interfaces. Beyond  $200 \text{ mV s}^{-1}$ , the voltammetric shapes deviate from rectangular shapes which are related with the resistive components of the capacitor cell. It can be noticed from figure 4(B), that a fading of  $\sim 20\%$  in specific capacitance as a function of scan rates (up to  $500 \text{ mV s}^{-1}$ ) has been observed, which is possibly associated with the diffusional limitations of the ions through the pores of tw-AC electrodes. The residual specific capacitance (after fading) at higher scan rates is still  $\sim 208 \text{ F g}^{-1}$  for the cell which is owing to the double-layer formation through the meso-pores of the tw-AC electrodes.

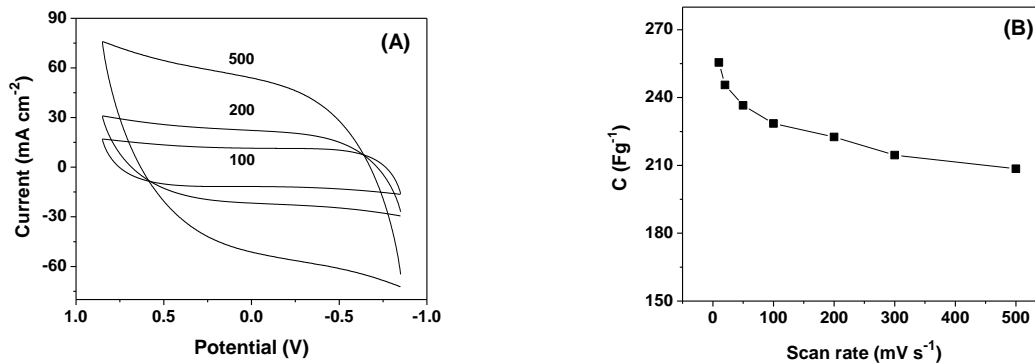


**Figure 4.** (A) CV response of solid-state EDLC cell at different scan rates (scan rates in  $\text{mV s}^{-1}$  are marked on each curve); and (B) variation of the specific capacitance values as a function of scan rate for the corresponding EDLC cell.

### 3.6. Galvanostatic charge-discharge

The charge-discharge studies have been carried out with different current densities varying from  $1.0 \text{ mA cm}^{-2}$  to  $6.0 \text{ mA cm}^{-2}$ . Figure 5(A) shows typical discharge characteristics of the EDLC cell at different current loads from  $1.0$  to  $4.0 \text{ mA cm}^{-2}$ . The discharge characteristics of the cell for each value of current load have been found to be close to linear variation (figure 5A), which confirms the capacitive nature of the EDLC cells. The internal resistance of each cell, which is also referred as equivalent series resistance (*ESR*), has been evaluated from the initial sudden drop in voltage, observed in discharge characteristics of each cell. This voltage drop during constant current discharge is the ohmic drop across the *ESR* of the capacitor cell. The values of discharge capacitance  $C_d$  are evaluated from the linear part of the discharge characteristics using equation (3). The values of *ESR* and discharge capacitance  $C_d$  of different EDLC cells are given in Table 3. The  $C_d$  and *ESR* values, observed from this charge-discharge method, have been found to be almost comparable to the capacitance values and *ESR* obtained from the EIS studies. There are few reports, in which the combination of bulk resistance  $R_b$ , and charge transfer resistance  $R_{ct}$ , (from EIS studies) is treated as *ESR* for the calculation of power density values, however, such values never matches (as in the present case also) with the values of *ESR* evaluated from galvanostatic charge-discharge tests.

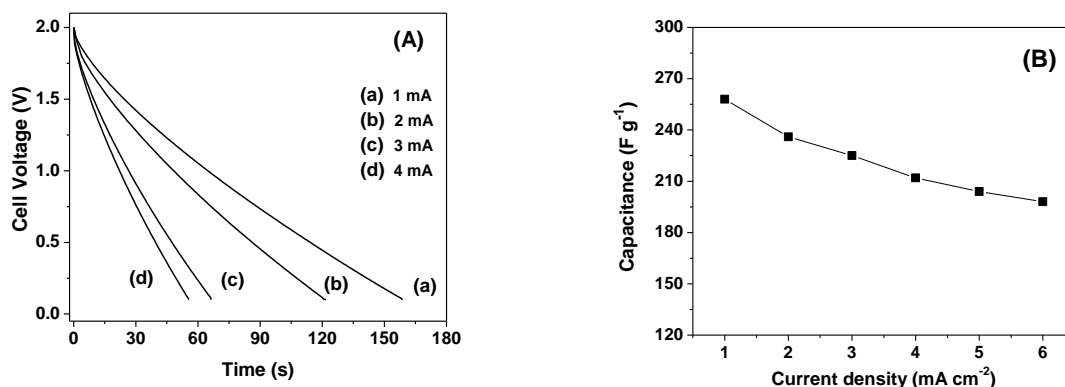


**Figure 5.** (A) Discharge curves of the solid-state EDLC cell at different constant current loads of  $1.0$ ,  $2.0$ ,  $3.0$ , and  $4.0 \text{ mA cm}^{-2}$ ; and (B) variation of the discharge capacitance as a function of current density of the corresponding EDLC cell.

Figure 5 (B) shows the variation of capacitance values of the EDLC cell as a function of applied current loads. A slight capacitance fading up to a value of  $6 \text{ mA cm}^{-2}$  of current density has been observed for the cell, which shows that these devices are suitable to be used as power sources, alternative to the rechargeable batteries, especially for low energy density applications.

The specific energy and power density of the capacitor cell has also been evaluated using the following expressions:

$$E = \frac{CV^2}{2m} \text{ and } P = \frac{V^2}{4m \cdot ESR} \quad (4)$$

respectively, where  $C$  is in farad,  $V$  is the voltage excluding the  $iR$  drop, and  $m$  is the mass of the activated carbon powder used in the single electrode. The values of specific energy and power density for the present supercapacitor cell are found to be  $36 \text{ W h kg}^{-1}$  and  $33 \text{ kW kg}^{-1}$ , respectively (Table 3). These values are comparable to the values reported in the literature [20,38,39].

**Table 3.** Typical charge–discharge characteristics of EDLC cell at a constant current density  $1 \text{ mA cm}^{-2}$ .

ESR ( $\Omega \text{ cm}^2$ )	Discharge Capacitance, $C_d$ ( $\text{F g}^{-1}$ )	Specific Energy, $E$ ( $\text{W h kg}^{-1}$ )	Power Density, $P$ ( $\text{kW kg}^{-1}$ )
$\sim 30$	$\sim 258$	$\sim 36$	$\sim 33$

Figure 6 (A) shows the variation of the specific power with respect to the specific energy (Ragone plots) of the EDLC cell. The power density-specific energy relationship of the cell shows a typical knee shape. Finally, the EDLC cells were tested for prolonged charge-discharge cycles. Figure 6 (B) shows the variation of specific capacitance of the EDLC cell as a function of galvanostatic charge-discharge cycles. The capacitance values of the cell have been found to be stable for  $\sim 10,000$  cycles after initial fading in capacitance values. It may be noted that for the few initial cycles there is about 20% decrement in the capacitance value for EDLC cell which may be due to two possible reasons (i) some charges are consumed possibly in irreversible reaction with loosely bound ions (most probably  $\text{OH}^-$  groups) adsorbed onto the electrode surface, and/or (ii) during charging, some micro-pores of the tw-AC electrodes have the possibility to be blocked permanently. However, even after initial decrease, stable and substantially high capacitance values  $\sim 205 \text{ F g}^{-1}$  for the cell has been obtained up to 10,000 charge-discharge cycles.

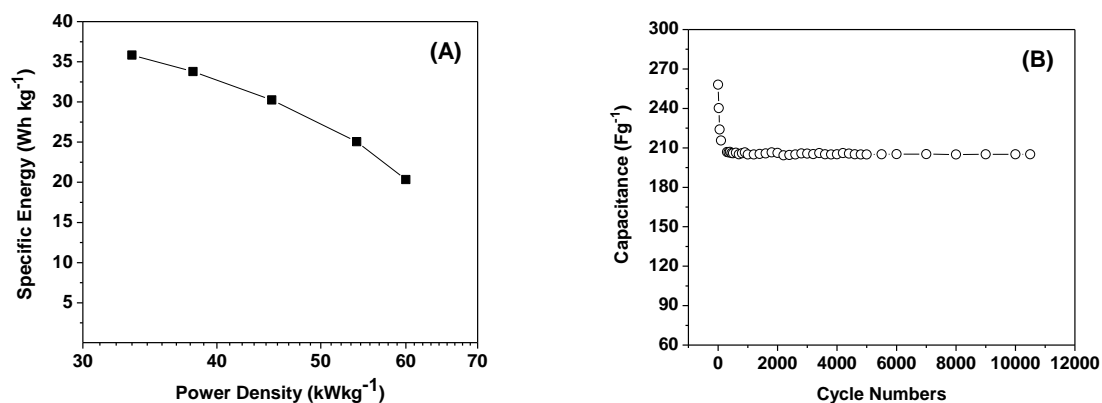


**Figure 6.** (A) Ragone plot for the solid-state EDLC cell; and (B) variation of the discharge capacitance of EDLC cell, evaluated at constant current load of  $1.0 \text{ mA cm}^{-2}$ , as a function of charge-discharge cycles.

#### 4. Conclusion

EIS, CV and charge-discharge studies on a novel configuration of EDLCs have been reported with plastic crystalline succinonitrile-based gel polymer electrolytes and the tw-AC electrodes. The specific activation process has been adopted to obtain the cost-effective activated carbon powder of specific surface area of  $\sim 1700 \text{ m}^2\text{g}^{-1}$  with the substantial proportion of meso-porosity for the fabrication of high performance EDLCs. The electrochemical properties of GPE films possessing the room temperature ionic conductivity of the order of  $10^{-3} \text{ S cm}^{-1}$  and wide enough electrochemical stability window show their suitability for EDLC applications. The EDLC cell offers promising values of  $\sim 270 \text{ F g}^{-1}$ ,  $\sim 36 \text{ Wh kg}^{-1}$ , and  $\sim 33 \text{ kW kg}^{-1}$  for specific capacitance, energy density, and power density, respectively. These values are comparable to those of many EDLCs, recently, reported in the literature.

#### Acknowledgments

We acknowledge the grants from the *Ministry of Science, Technology and Innovation* (MOSTI) (03-01-02-SF1118) and *Universiti Kebangsaan Malaysia* (DIP-2014-027) and the support of CRIM (Centre for Research and Innovation Management), UKM. The authors also thank to Mr. Saini for help with the laboratory work and for the collaborative work of Department of Physics and Astrophysics, University of Delhi, India.

#### References

- [1] Conway B E 1999 *Electrochemical Supercapacitors: Scientific Fundamentals and Technological Applications* (Kluwer Academic/Plenum Publishers, New York)
- [2] Kotz R and Carlen M 2000 *Electrochim. Acta* **45** 2483
- [3] Simon P and Gogotsi Y 2008 *Nat. Mater.* **7** 845
- [4] Hashmi S A 2004 *Natl. Acad. Sci. Letts.* **27** 27
- [5] Ghosh A and Lee Y H, 2012 *Chem. Sus. Chem.* **5** 480
- [6] Barbieri O, Hahn M, Herzog A, Kotz R 2005 *Carbon* **43** 1303
- [7] He X, Lei J, Geng Y, Zhang X, Wu M and Zheng M 2009 *J. Phys. Chem. Solids* **70** 738
- [8] Xia X H, Shi L, Liu H B, Yang L and He Y D 2012 *J. Phys. Chem. Solids* **73** 385
- [9] Hu Z and Srinivasan M P 1999 *Micropor. Mesopor. Mater.* **27** 11
- [10] Xing W, Qiao S Z, Ding R G, Li F, Lu G Q, Yan Z F and Cheng H M 2006 *Carbon* **44** 216
- [11] Huang C W, Hsu C H, Kuo P L, Hsieh C T and Teng H 2011 *Carbon* **49** 895
- [12] Xiong W, Liu M, Gan L, Lu Y, Li Y, Yang L, Xu Z, Hao Z, Liu H and Chen L 2011 *J. Power Sources* **196** 10461
- [13] Nor N S M, Deraman M, Omar R, Awitdrus, Farma R, N H Basri, B. N. M. Dolah, N. F. Mamat, B. Yatim and M. N. M. Daud 2015 *Energy* **79** 183
- [14] Dolah B N M, Deraman M, Othman M A R, Farma R, Taer E, Awitdrus, Basri N H, Talib I A, Omar R and Nor N S M 2014 *Mater. Res. Bull.* **60** 10
- [15] Farma R, Deraman M, Awitdrus A, Talib I A, E Taer, Basri N H, Manjunatha J G, Ishak M M, Dollah B N M and Hashmi S A 2013 *Bioresour. Technol.* **132** 254
- [16] Basri N H, Deraman M, Kanwal S, Talib I A, Manjunatha J G, Aziz A A and Farma R 2013 *Biomass Bioenerg.* **59** 370
- [17] Taer E, Deraman M, Talib I A, Awitdrus A, Hashmi S A and Umar A A 2011 *Int. J. Electrochem. Sci.* **6** 3301
- [18] Hu Z, Srinivasan M P and Ni Y 2000 *Adv. Mater.* **12** 62
- [19] Hu Z and Srinivasan M P 1999 *Micropor. Mesopor. Mater.* **27** 11
- [20] Suleman M, Kumar Y and Hashmi S A 2015 *J. Solid State Electrochem.* **19** 1347
- [21] Song J Y, Wang Y Y and Wan C C 1999 *J. Power Sources* **77** 183
- [22] Agrawal R C and Pandey G P 2008 *J. Phys D Appl. Phys.* **41** 223001
- [23] P J Alarco, Lebdeh Y A, Abouimrane A and Armand M 2004 *Nat. Mater.* **3** 476
- [24] MacFarlane D R and Forsyth M 2001 *Adv. Mater.* **13** 957
- [25] Fan L Z and Maier J 2006 *Electrochem. Comm.* **8** 1753

- [26] Patel M, Chandrappa K G and Bhattacharyya A J 2008 *Electrochim. Acta* **54** 209
- [27] Patel M, Chandrappa K G and Bhattacharyya A J 2010 *Solid State Ion.* **181** 844
- [28] Suleman M, Kumar Y and Hashmi S A 2013 *J. Phys. Chem. B.* **117** 7436
- [29] Masui A, Yoshioka S and Kinoshita S 2001 *Chem. Phys. Lett.* **341** 299
- [30] Derollez P, Lefebvre J, Descamps M, Press W and Fontaine H 1990 *J. Phys-Condens. Mat.* **2** 6893
- [31] Zhou J, Cai J, Cai S, Zhou X and Mansour A N 2011 *J. Power Sources* **196** 10479
- [32] Kumar D, Suleman M and Hashmi S A 2011 *Solid State Ion.* **202** 45
- [33] Chen H, Wang F, Tong S, Guo S and Pan X 2012 *Appl. Surf. Sci.* **258** 6097
- [34] Marsh H and Reinoso F R 2006 *Activated Carbon* (1<sup>st</sup> edn, Elsevier Science Tech. Books) p 1-554
- [35] Sheng K X, Sun Y Q, Li C, Yuan W J and Shi G Q 2012 *Sci. Rep.* **2** 247
- [36] Pandolfo A G and Hollenkamp A F 2006 *J. Power Sources* **157** 11
- [37] Kim T Y, Jung G, Yoo S, Suh K S and Ruoff R S 2013 *ACS Nano* **7** 6899
- [38] G.P. Pandey, A.C. Rastogi and C. R. Westgate 2014 *J. Power Sources* **245** 857
- [39] Pandey G P and Hashmi S A 2013 *Electrochim. Acta* **105** 333
- [40] Miller J R 1998 *Proc. of the Eighth International Seminar on Double layer Capacitors and Similar Energy Storage Devices* (Deerfield Beach, Florida, USA) p 21